Electronic Supplementary Material (ESI) for Journal of Materials Chemistry A.

Electronic Supplementary Information (ESI)

A micro/nano multiscale hierarchical structure strategy to fabricate highly conducting films for electromagnetic interference shielding and energy storage

Beibei Wang[1,4], Weiye Zhang[1,4], Jingmeng Sun[1,4], Chenhuan Lai[2], Shengbo Ge[2], Hongwu Guo[1,4]*, Yi Liu[1,4]*, Daihui Zhang[2,3]*

[1]Key Laboratory of Wood Material Science and Application (Beijing Forestry University), Ministry of Education, Beijing 100083, China

[2]Co-Innovation Center of Efficient Processing and Utilization of Forest Resources, Nanjing Forestry University, Nanjing 210037, Jiangsu, China

[3]Institute of Chemical Industry of Forest Products, Chinese Academy of Forestry, Nanjing, Jiangsu 210042, China

[4]Engineering Research Center of Forestry Biomass Materials and Energy, Ministry of Education，Beijing Forestry University, Beijing 100083, China

*Corresponding author. E-mail: guohongwu_305@bjfu.edu.cn, liuyichina@bjfu.edu.cn, Daihui.zhang@mail.mcgill.ca

Figures

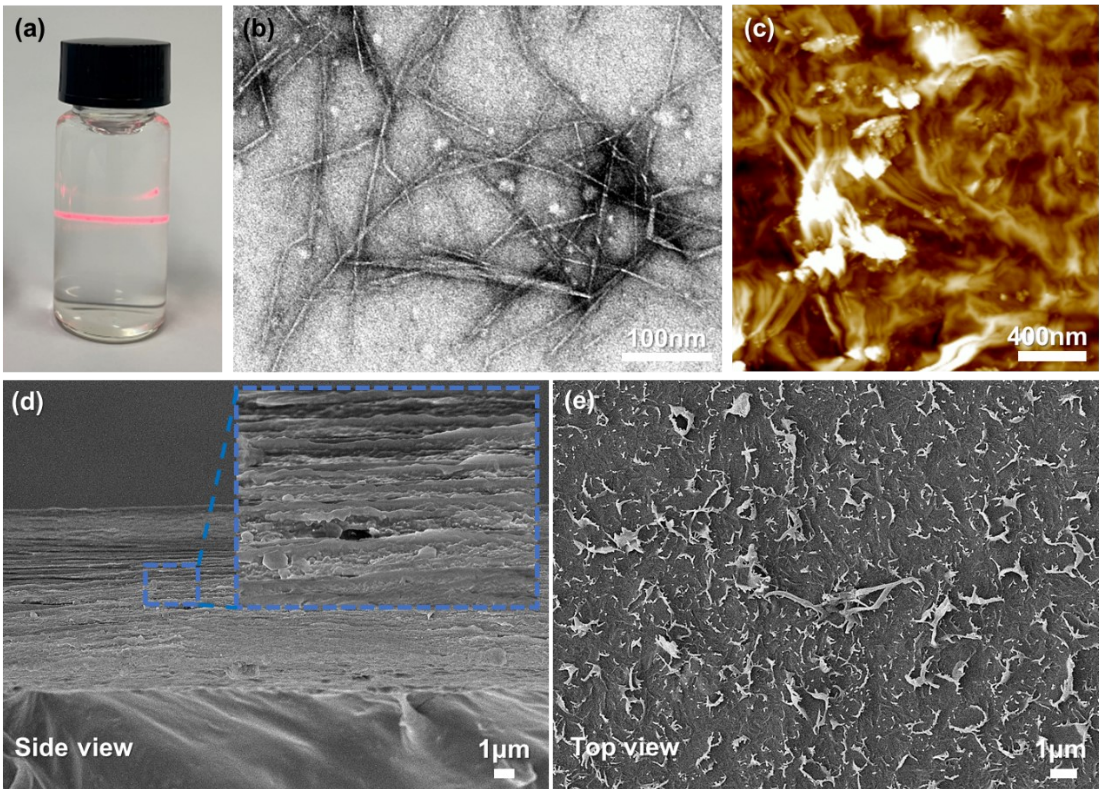

Fig. S 1 a Digital photograph of the TOCNFs suspension. **b** TEM image of the TOCNFs suspension. **c** AFM image of the TOCNFs suspension. **d-e** Side view and top view of the pure TOCNFs film

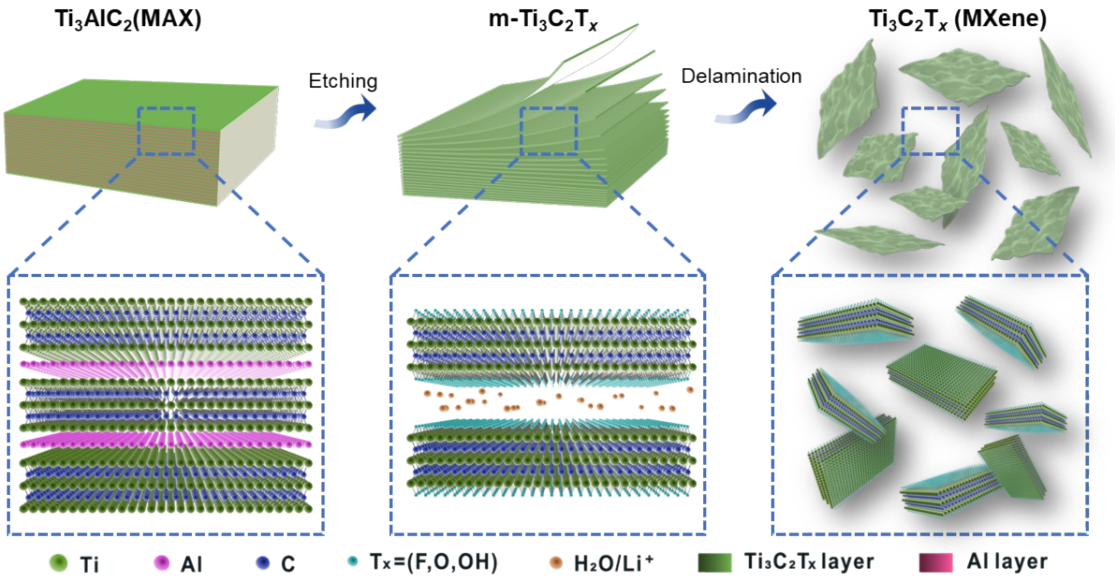

Fig. S 2 Schematic illustration of the preparation of $Ti_3C_2T_x$ nanosheets

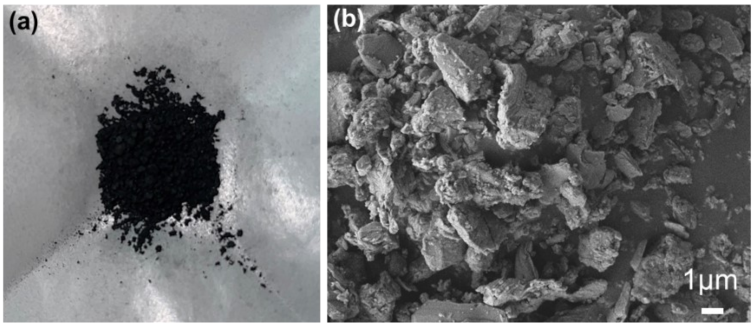

Fig. S 3 a Digital photograph. **b** SEM image of the MAX powder

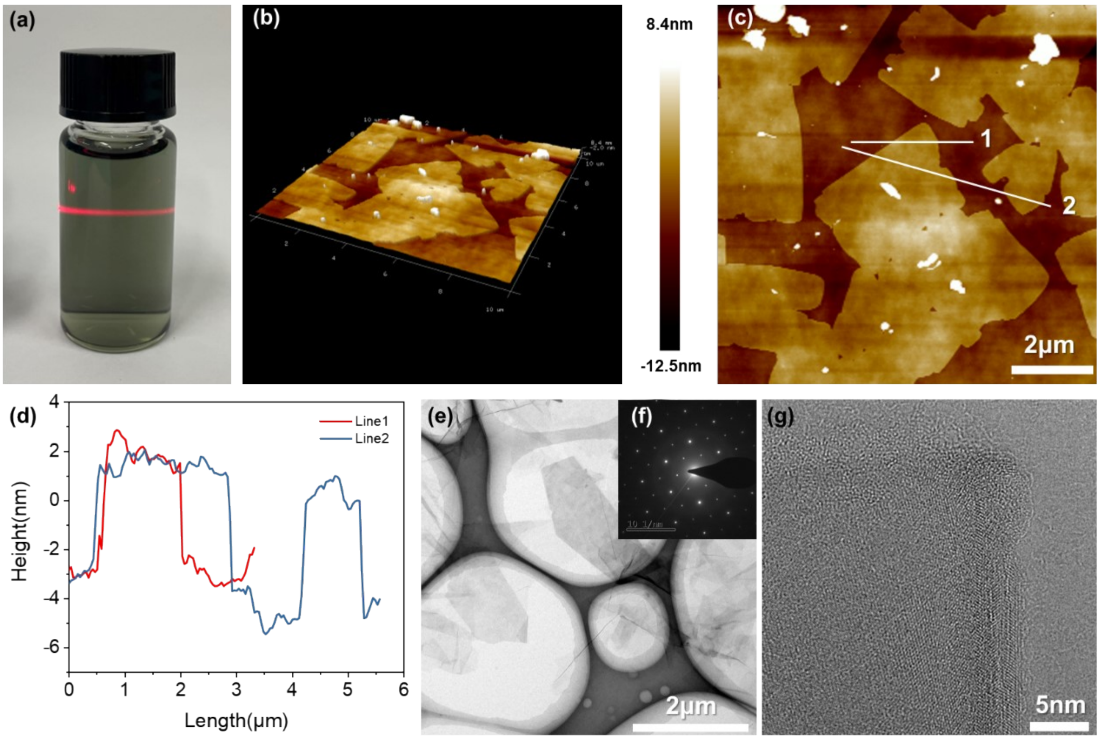

Fig. S 4 a Digital photograph of the $Ti_3C_2T_x$ suspension. **b** AFM image of the $Ti_3C_2T_x$ suspension. **c** AFM image of the $Ti_3C_2T_x$ nanosheets. **d** Height profiles of the different lines marked on **c**. **e** HR-TEM image of the $Ti_3C_2T_x$ suspension. **f** SAED patterns, and **g** lattice fringes

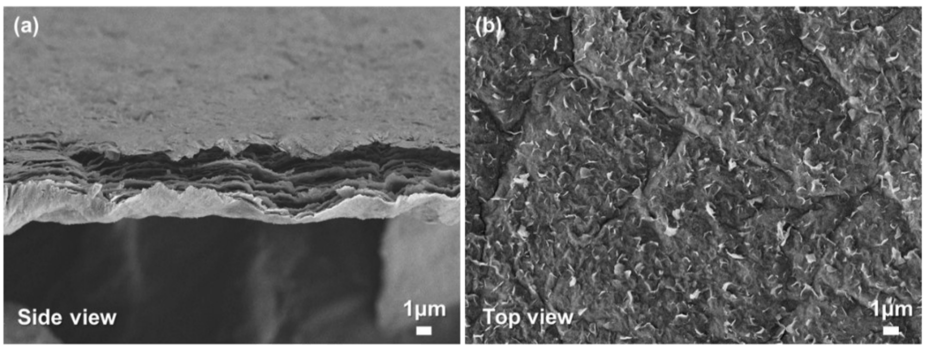

Fig. S 5 a side view and **b** top view of the pure $Ti_3C_2T_x$ film

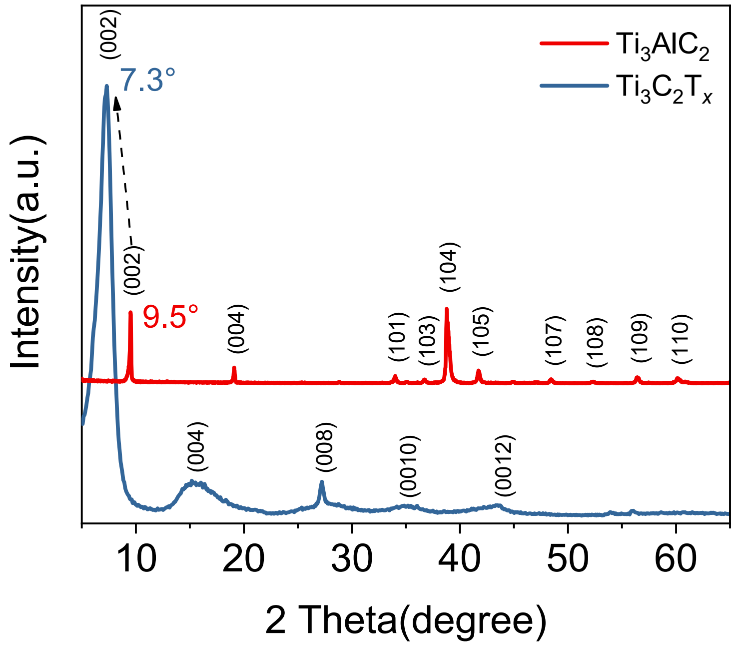

Fig. S 6 XRD patterns of Ti_3AlC_2 and $Ti_3C_2T_x$

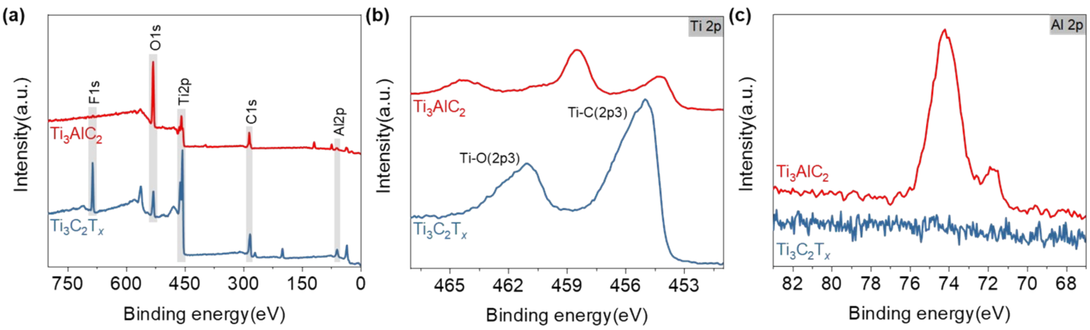

Fig. S 7 a XPS wide-scan spectra, **b** Ti 2p spectra, and **c** Al 2p spectra of the Ti_3AlC_2 precursor and the $Ti_3C_2T_x$ nanosheets

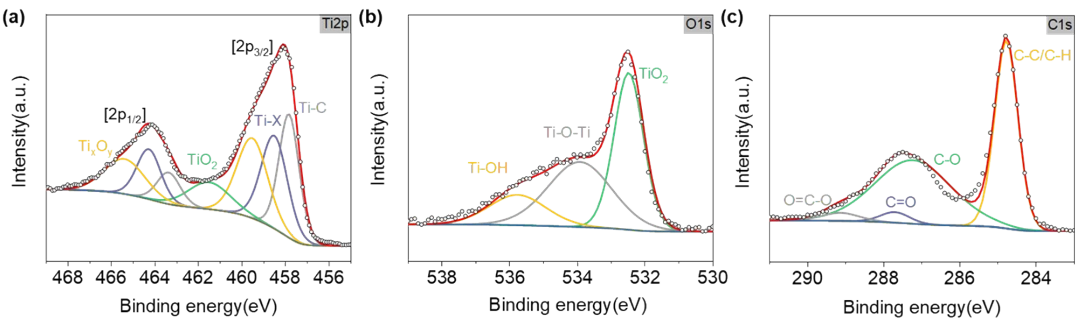

Fig. S 8 a Ti 2p, **b** O 1s, and **c** C 1s spectra of $Ti_3C_2T_x$

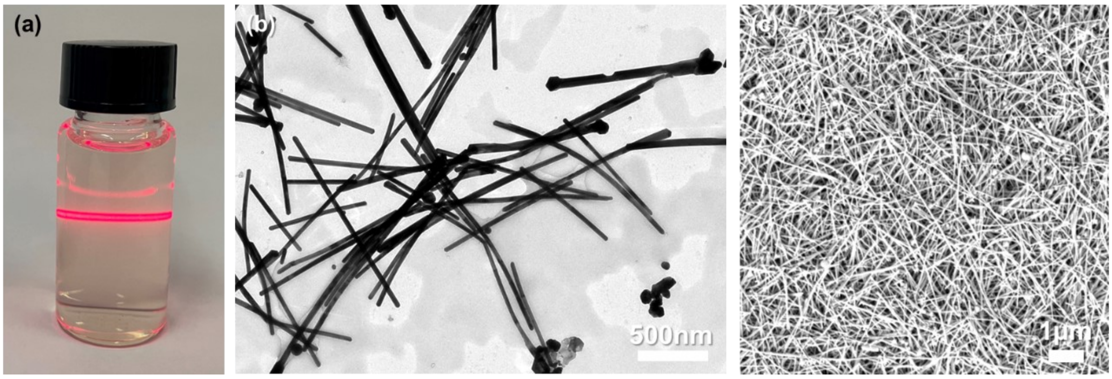

Fig. S 9 **a** Digital photograph of the AgNW suspension. **b** TEM image of AgNW suspension, and **c** SEM image of the pure AgNW film

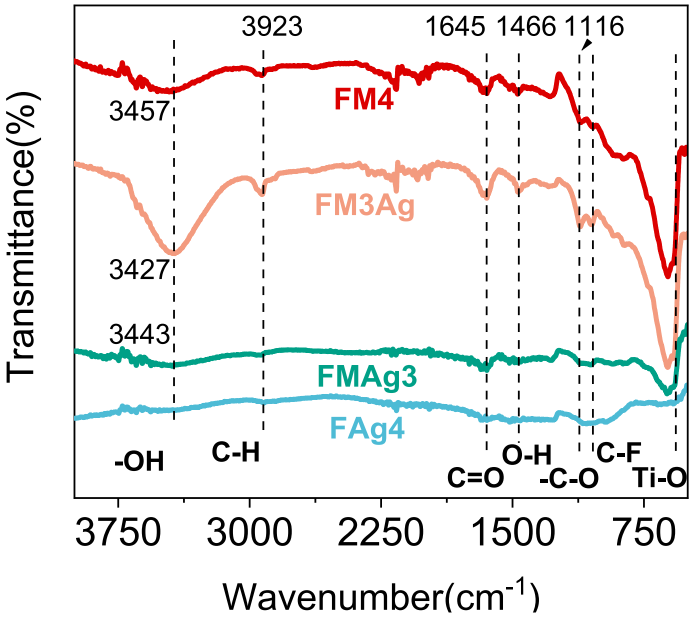

Fig. S 10 FT-IR spectra of FM4, FM3Ag, FMAg3, and FAg4 hybrid films

The FM4 had a vibrational mode at 3482 cm^{-1} assigned for -OH group out-of-plane vibration, 1038 cm^{-1} for C-F bonds, and 573 cm^{-1} for Ti-O bonds. For FAg4, obvious absorption peaks are observed at 1079 cm^{-1}, and 1746 cm^{-1} for -C-O bonds and almost had indistinct -OH vibrational peaks.

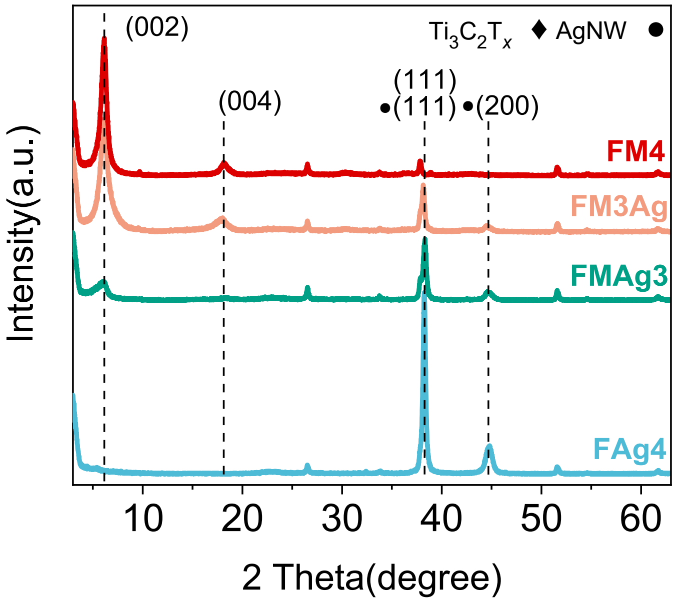

Fig. S 11 XRD patterns of FM4, FM3Ag, FMAg3, and FAg4 hybrid films

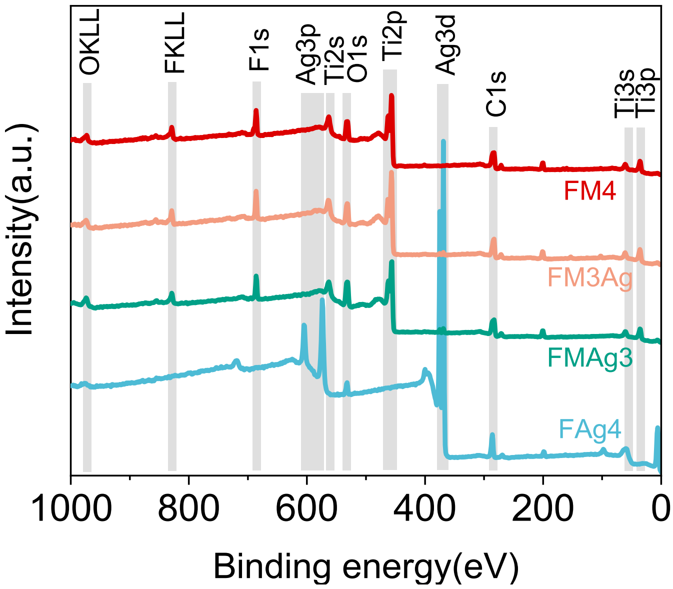

Fig. S 12 XPS survey scan spectra of FM4, FM3Ag, FMAg3, and FAg4 hybrid films

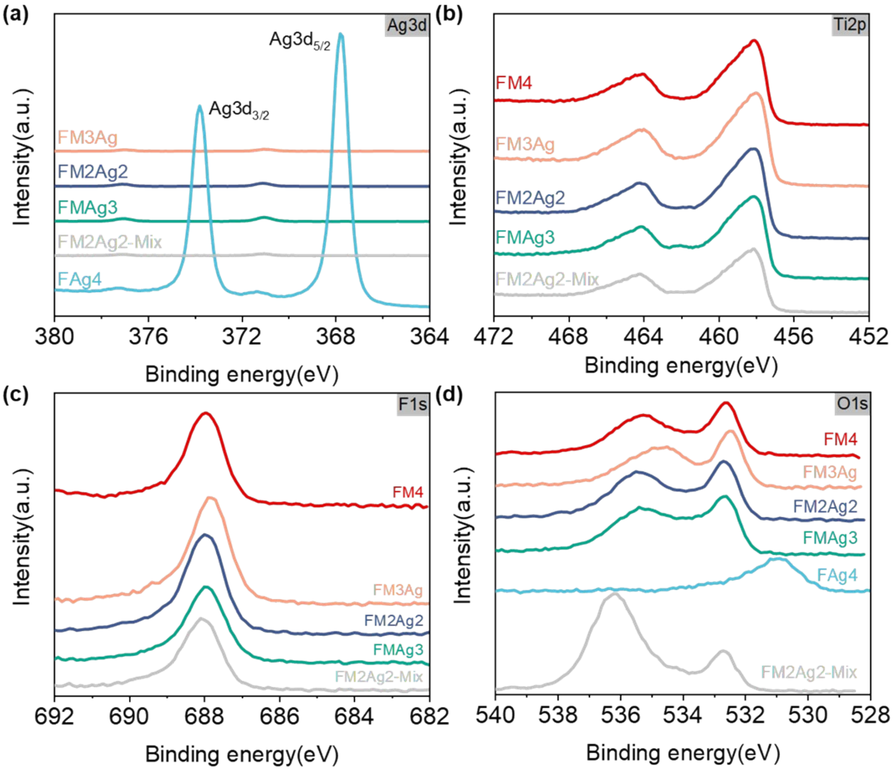

Fig. S 13 High-resolution XPS from **a** Ag 3d region, **b** Ti 2p region, **c** F 1s region and **d** O 1s region of the TOCNFs/$Ti_3C_2T_x$/AgNW hybrid films

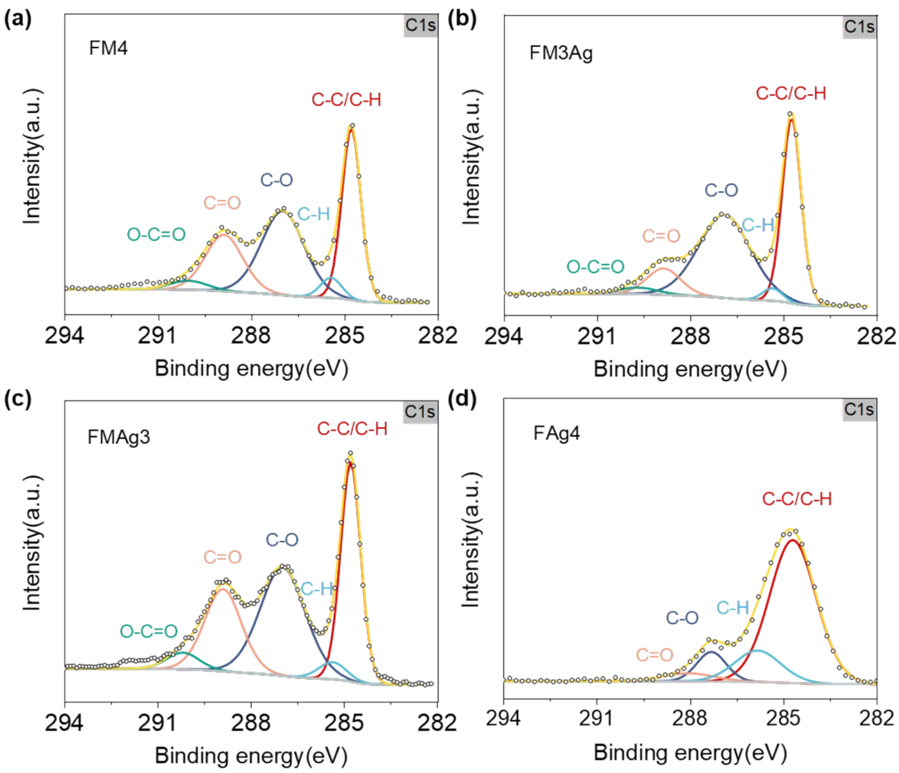

Fig. S 14 C 1s spectra of **a** FM4, **b** FM3Ag, **c** FMAg3, and **d** FAg4

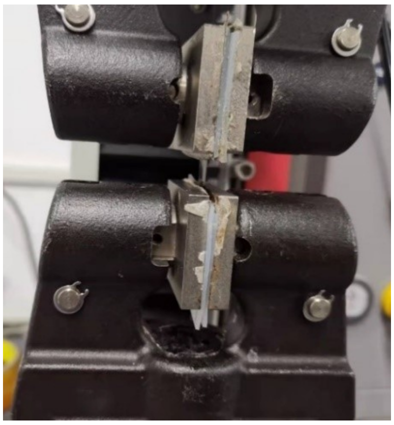

Fig. S 15 Digital photo of micromechanical test

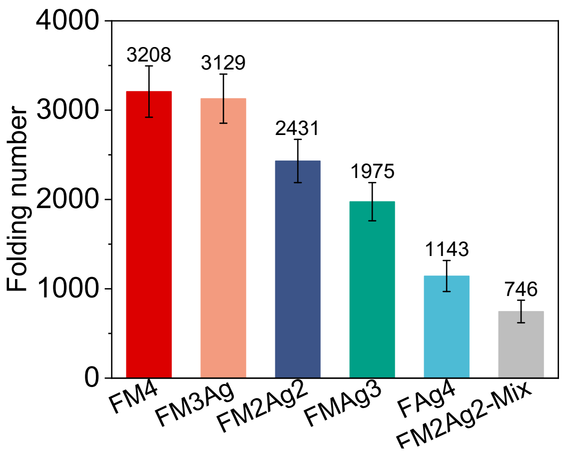

Fig. S 16 Folding times of the TOCNFs/$Ti_3C_2T_x$/AgNW hybrid films under loading of 4.9 N

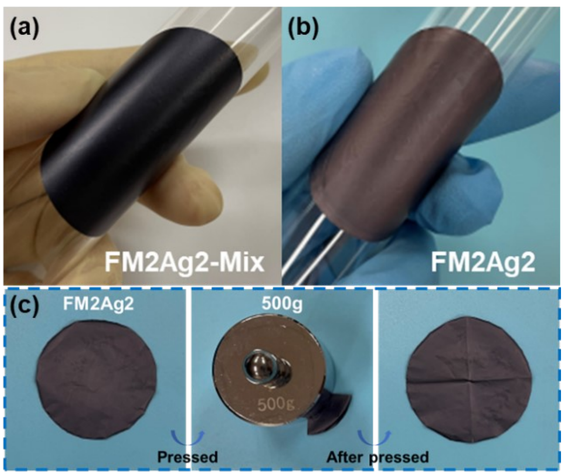

Fig. S 17 Digital photos of **a** FM2Ag2-Mix hybrid film, **b** FM2Ag2 hybrid film, and **c** FM2Ag2 hybrid film loaded with a weight of 500 grams without breaking or cracking

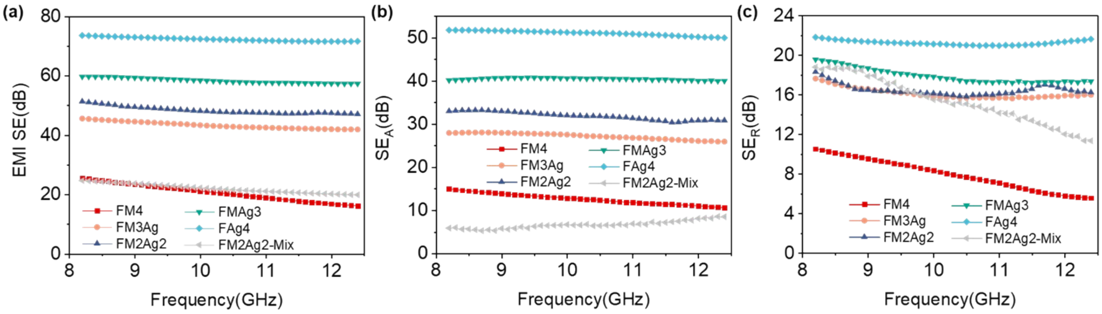

Fig. S 18 a EMI SE of the TOCNFs/$Ti_3C_2T_x$/AgNW hybrid films in the X-band region. **b** SE_A, and **c** SE_R

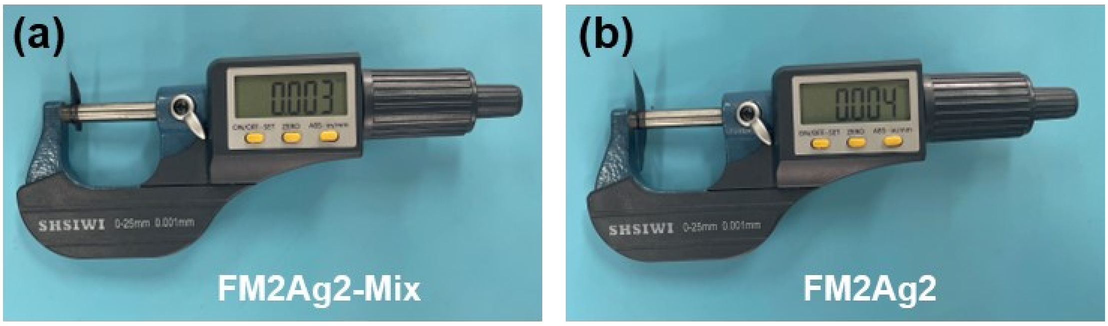

Fig. S 19 The thickness of the FM2Ag2-Mix and FM2Ag2 hybrid films

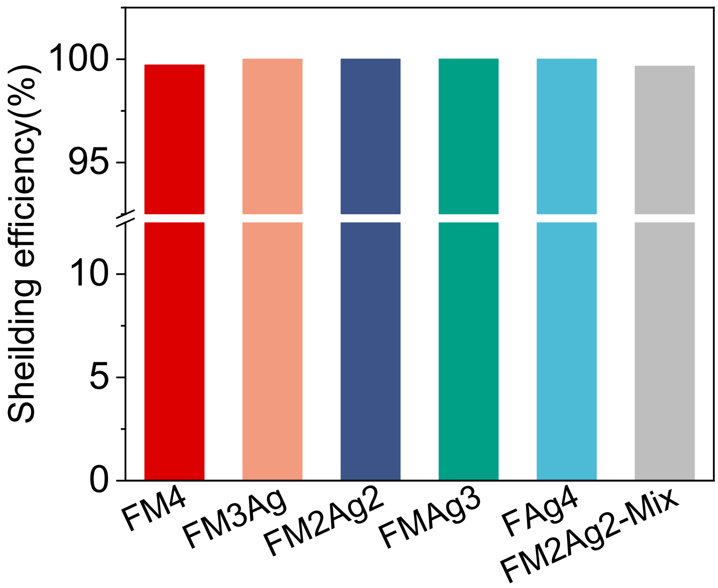

Fig. S 20 Shielding efficiencies of the TOCNFs/$Ti_3C_2T_x$/AgNW hybrid films

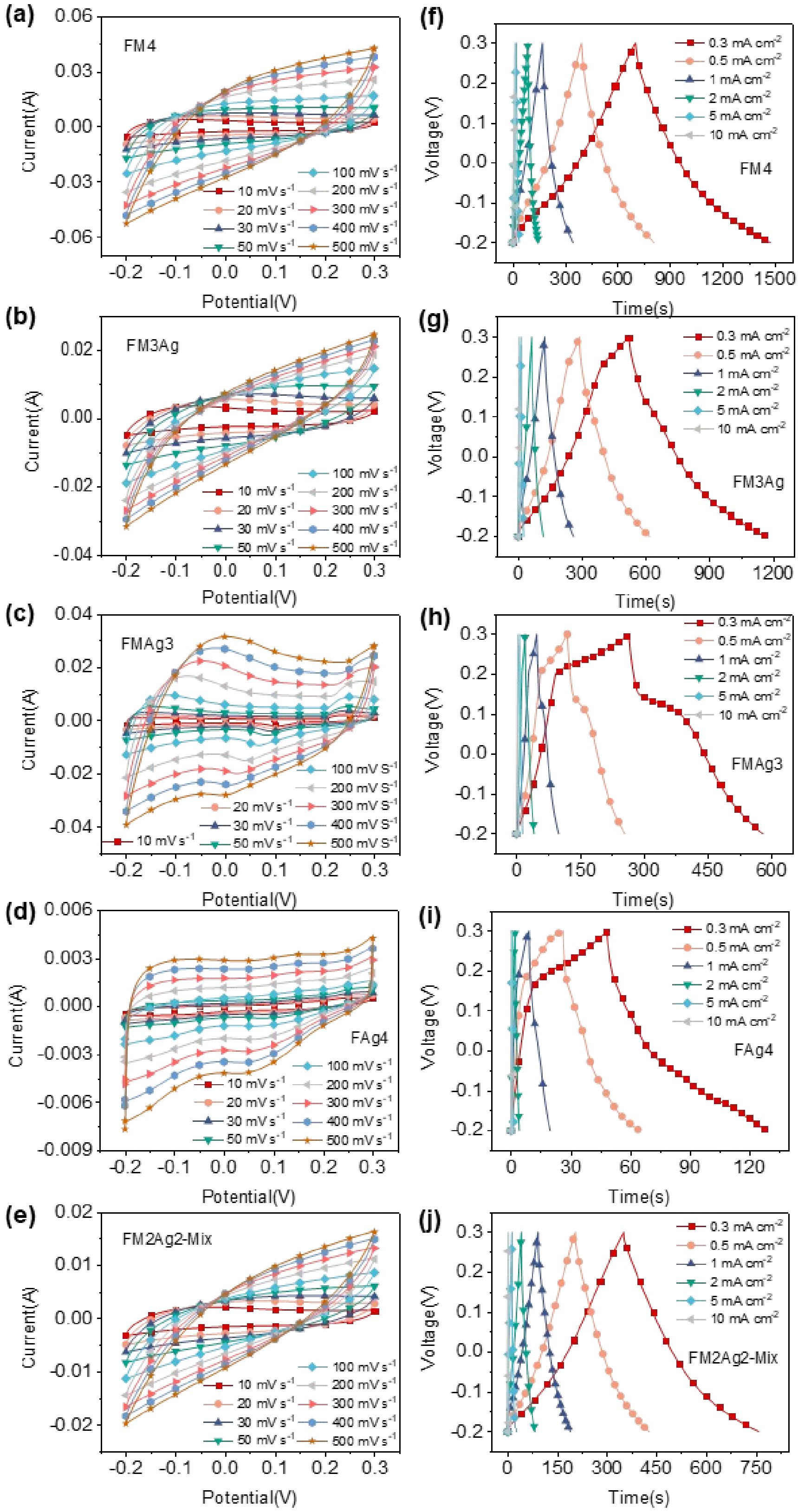

Fig. S 21 CV curves and GCD curves of the TOCNFs/$Ti_3C_2T_x$/AgNW electrodes: **a**,**f** FM4, **b**,**g** FM3Ag, **c**,**h** FMAg3, **d**,**i** FAg4, and **e**,**j** FM2Ag2-Mix at different current densities

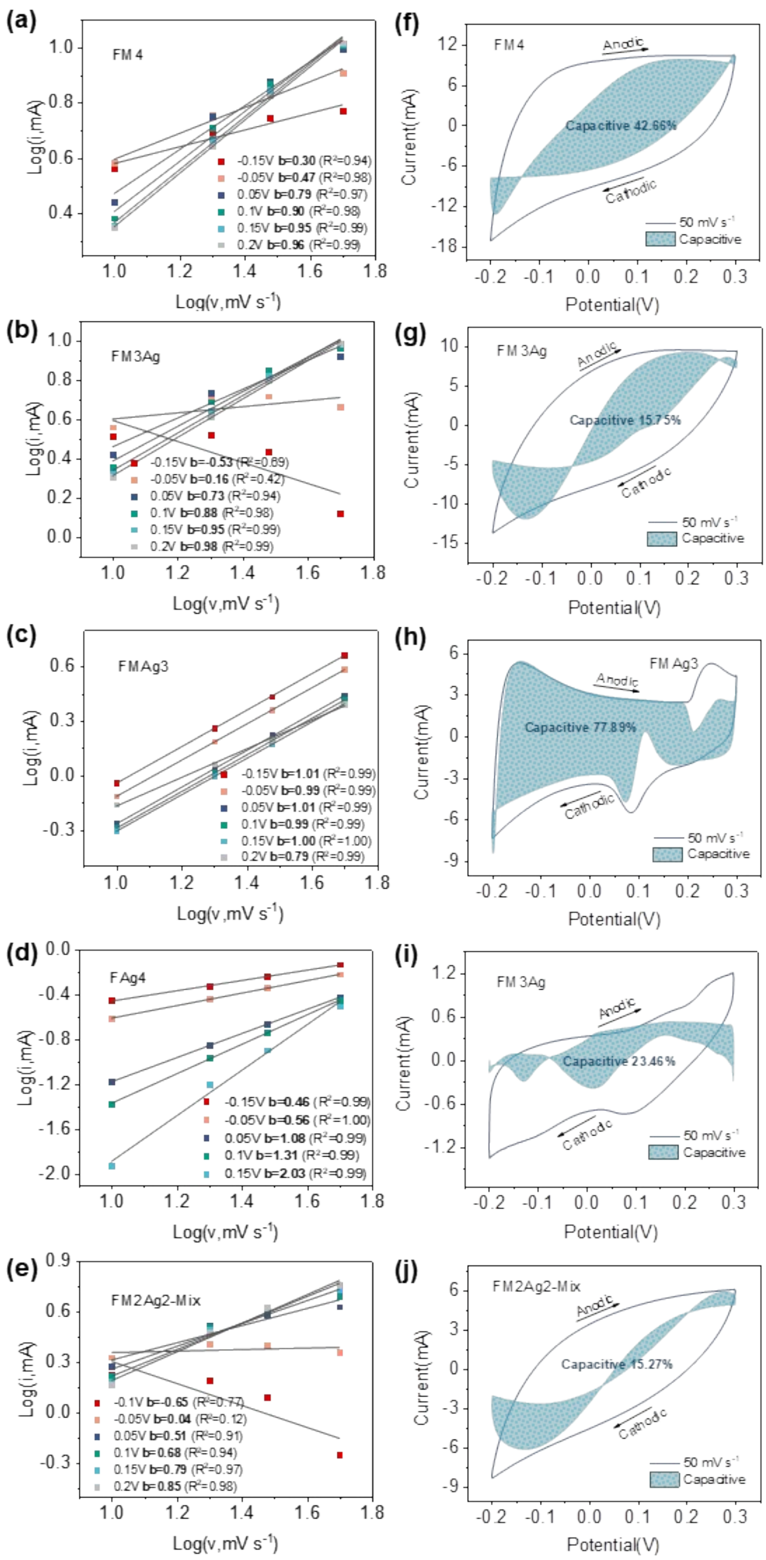

Fig. S 22 The liner relationship of the current (*i*) and the scan rate (*v*), and surface capacitance contribution of the TOCNFs/ $Ti_3C_2T_x$ /AgNW electrodes to the total charge storage at 50 mV s^{-1}: **a**,**f** FM4, **b**,**g** FM3Ag, **c**,**h** FMAg3, **d**,**i** FAg4, and **e**,**j** FM2Ag2-Mix

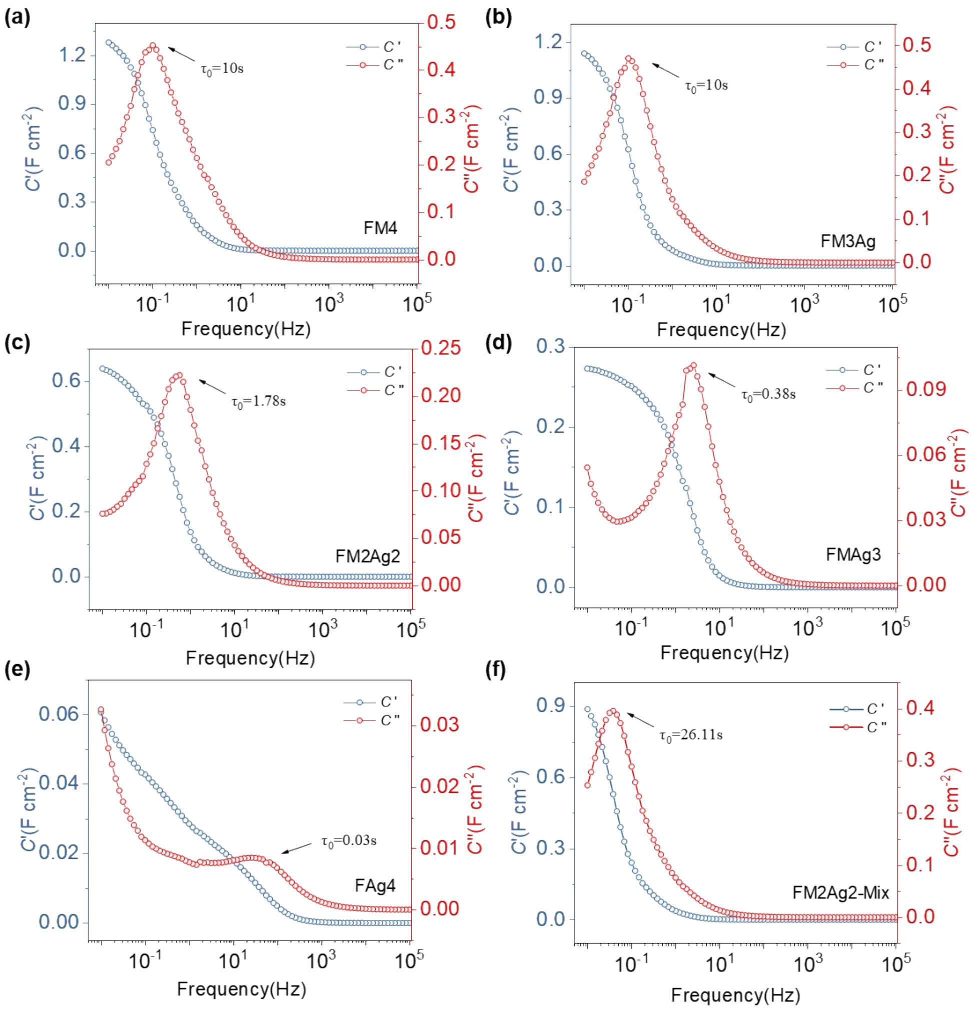

Fig. S 23 Normalized real (C') and imaginary (C'') parts of capacitance vs. frequency of the electrodes: **a** FM4, **b** FM3Ag, **c** FM2Ag2, **d** FMAg3, **e** FAg4, and **f** FM2Ag2-Mix

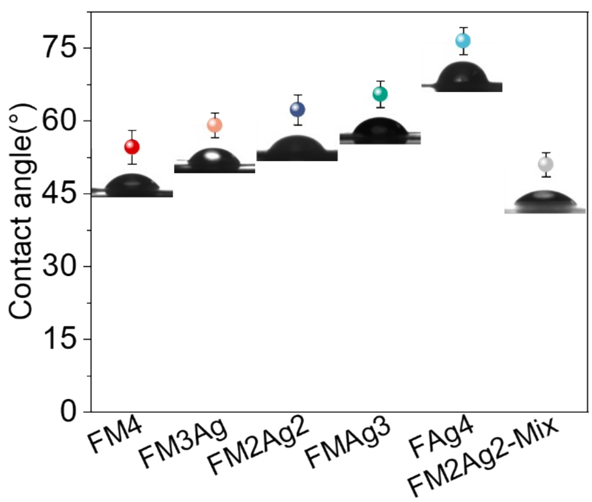

Fig. S 24 Contact angle of TOCNFs/$Ti_3C_2T_x$/AgNW hybrid films

Tables

Table S1 The mechanical properties of the TOCNFs/$Ti_3C_2T_x$/AgNW hybrid films with different $Ti_3C_2T_x$/AgNW contents

Sample	Tensile strength (MPa)	Fracture strain (%)	Toughness (MJ/m^3)	Young's modulus (GPa)
FM4	116.10 ± 8.19	2.85 ± 0.26	1.09 ± 0.08	9.02 ± 0.69
FM3Ag	107.41 ± 8.27	1.42 ± 0.20	0.68 ± 0.05	11.20 ± 0.85
FM2Ag2	85.63 ± 7.24	2.48 ± 0.24	1.02 ± 0.10	5.18 ± 0.29
FMAg3	76.89 ± 7.14	2.26 ± 0.27	0.94 ± 0.07	5.03 ± 0.31
FAg4	49.48 ± 5.67	1.74 ± 0.18	0.33 ± 0.07	4.55± 0.67
FM2Ag2-Mix	40.95 ± 5.29	1.57 ± 0.15	0.41 ± 0.08	3.98 ± 0.53

Table S2 Comparison of the EMI shielding performance of the TOCNFs/$Ti_3C_2T_x$/AgNW hybrid films and other materials

Sample	Materials	Thickness (μm)	Conductivity (S m^{-1})	EMI SE (dB)	SSE/t (dB cm^2 g^{-1})	References
1	CNF/CNT/$Ti_3C_2T_x$	12	365000	20.5	9316.4	[1]
2	Ag@CMS	1000	5.47×10^{-5}	107.5	853.3	[2]
3	Ag nanowires	5000	5.4×10^{-8}	35	2416	[3]
4	CNTs/Ti_3C_2 MXene/CNFs	38	2506.6	38.4	8020	[4]
5	d-$Ti_3C_2T_x$/CNFs	167	9.691	25	1326	[5]
6	BMF/AgNW/MXene	2000	24.5	52.6	5313	[6]
7	MXene/AgNW/PU	1320	0.025	59	23674	[7]
8	PVDF/MXene/AgNW	300	1.08	25.87	1091	[8]
9	CNF@MXene@AgNW	85	37378.2	55.9	10647.6	[9]
10	MXene/AgNW	16.9	30000	42.7	16724	[10]
11	graphene/PDMS foam	1000	2	30	500 dB cm^3 g^{-1}	[11]
12	FM4	4	1050000 ± 135000	25.49	13918.31	
13	FM3Ag	4	8400000 ± 250000	45.57	24883.45	**This work**
14	FM2Ag2	4	12900000 ± 280000	51.30	28016.19	

15	FMAg3	4	18100000 ± 290000	59.70	32599.35
16	FAg4	5	27700000 ± 320000	73.55	40165.72
17	FM2Ag2-Mix	3	398000 ± 115000	24.67	13474.13

Table S3 Comparison of electrochemical performance of electrodes between this work and the published works on MXene hybrids

Sample	Materials	Scan rate	Specific capacitance (F g^{-1})	Areal capacitance (mF cm^{-2})	Stability	References
1	Carbonized MXene/Cotton	2 mV s^{-1}	233.6	794.2	74% (10000 cycles)	12
2	MXene/ZnO	2 mV s^{-1}	120	233	86% (10000 cycles)	13
3	rGO/Ti_3C_2 composite aerogel	1 mA cm^{-2}	-	41	~100% (1500 cycles)	14
4	Polyester@MXene	5 mV s^{-1}		18.39	98.2% (6000 cycles)	15
5	CNF/CNT/$Ti_3C_2T_x$	0.3 mA cm^{-2}	279.7	537	93.1% (8000 cycles)	1
6	MXene/CNF	2 mV s^{-1}	285	25.3	100% (10000 cycles)	15
7	MXene ($Ti_3C_2T_x$)/ CNF/PC	0.1 mA cm^{-2}	-	143	90% (10000 cycles)	17
8	SF-MXene	10 mV s^{-1}	380	-	94% (10000 cycles)	18
9	$Ti_3C_2T_x$	5 mV s^{-1}	273	-	88.6% (10000)	19
10	$Ti_3C_2T_x$/Ag NP	2 mV s^{-1}	-	332.2	87% (10000)	20
11	FM2Ag2	10 mV s^{-1}	77.6	110.7	92.4% (10000)	This work
12	FM2Ag2-Mix	10 mV s^{-1}	73.5	104.9	78.6% (10000)	
13	FMAg3	10 mV s^{-1}	42.6	60.7	94.3% (10000)	
14	FAg4	10 mV s^{-1}	11.9	16.9	86.7% (10000)	

References

1 B. Wang, Y. Li, W. Zhang, J. Sun, J. Zhao, Y. Xu, Y. Liu, H. Guo and D. Zhang, *Carbohydr. Polym.*, 2022, **286**, 119302.

2 H. Zhang and J. Zhang, *J. Appl. Polym. Sci.*, 2020, **137**, 48459.

3 J. Ma, K. Wang and M. Zhan, *Rsc Adv.*, 2015, **5**, 65283-65296.

4 W. Cao, C. Ma, S. Tan, M. Ma, P. Wan and F. Chen, *Nano-Micro Lett.*, 2019, **11**, 270-286.

5 W. Cao, F. Chen, Y. Zhu, Y. Zhang, Y. Jiang, M. Ma and F. Chen, *Acs Nano*, 2018, **12**, 4583-4593.

6 C. Weng, G. Wang, Z. Dai, Y. Pei, L. Liu and Z. Zhang, *Nanoscale*, 2019, **11**, 22804-22812.

7 Y. Cheng, Y. Lu, M. Xia, L. Piao, Q. Liu, M. Li, Y. Zhou, K. Jia, L. Yang and D. Wang, *Compos. Sci. Technol.*, 2021, **215**, 109023.

8 H. Cheng, Y. Pan, Q. Chen, R. Che, G. Zheng, C. Liu, C. Shen and X. Liu, *Adv. Compos. Hybrid Mater.*, 2021, **4**, 505-513.

9 B. Zhou, Q. Li, P. Xu, Y. Feng, J. Ma, C. Liu and C. Shen, *Nanoscale*, 2021, **13**, 2378-2388.

10 M. Miao, R. Liu, S. Thaiboonrod, L. Shi, S. Cao, J. Zhang, J. Fang and X. Feng, *J. Mater. Chem. C*, 2020, **8**, 3120-3126.

11 Z. Chen, C. Xu, C. Ma, W. Ren and H. Cheng, *Adv. Mater.*, 2013, **25**, 1296-1300.

12 Y. Li, Z. Lu, B. Xin, Y. Liu, Y. Cui and Y. Hu, *Appl. Surf. Sci.*, 2020, **528**, 146975.

13 F. Wang, M. Cao, Y. Qin, J. Zhu, L. Wang and Y. Tang, *Rsc Adv.*, 2016, **6**, 88934-88942.

14 R. N, K. A, M. H. M, N. M. R, D. Mondal, S. K. Nataraj and D. Ghosh, *Appl. Surf. Sci.*, 2019, **481**, 892-899.

15 W. Shao, M. Tebyetekerwa, I. Marriam, W. Li, Y. Wu, S. Peng, S. Ramakrishna, S. Yang and M. Zhu, *J. Power Sources*, 2018, **396**, 683-690.

16 W. Tian, A. VahidMohammadi, M. S. Reid, Z. Wang, L. Ouyang, J. Erlandsson, T. Pettersson, L. Wågberg, M. Beidaghi and M. M. Hamedi, *Adv. Mater.*, 2019, **31**, 1902977.

17 W. Chen, D. Zhang, K. Yang, M. Luo, P. Yang and X. Zhou, *Chem. Eng. J.*, 2021, **413**, 127524.

18 L. Yin, H. Kang, H. Ma, J. Wang, Y. Liu, Z. Xie, Y. Wang and Z. Fan, *Carbon (New York)*, 2021, **182**, 124-133.

19 J. Wu, Q. Li, C. E. Shuck, K. Maleski, H. N. Alshareef, J. Zhou, Y. Gogotsi and L. Huang, *Nano Res.*, 2022, **15**, 535-541.

20 L. Li, N. Zhang, M. Zhang, L. Wu, X. Zhang and Z. Zhang, *Acs Sustain. Chem. Eng.*, 2018, **6**, 7442-7450.